SERBIAN JOURNAL OF ELECTRICAL ENGINEERING
Vol. 13, No. 3, October 2016, 381-394

UDC: 669.018.5:537.62 **DOI: 10.2298/SJEE1603381S**

Amorphous $Fe_{72}Cu_1V_4Si_{15}B_8$ Ribbon as Magneto-Impedance Sensing Element

Radoslav Surla[1], Nebojša Mitrović[1], Slobodan Đukić[1], Vedran Ibrahimović[2]

Abstract: Magneto-impedance (MI) effect in the $Fe_{72}Cu_1V_4Si_{15}B_8$ amorphous ribbon obtained by melt spinning method has been studied. The aim of study was the characterisation of this ribbon in as-cast state in terms of its application as a MI sensor. The experiments on MI elements were performed in the frequency range from 30 kHz to 300 MHz and maximum external magnetic field up to 28.6 kA/m. Maximum observed MI-ratio ($\Delta Z = Z(0) - Z(H_{max})$, $H_{max} = 28.6$ kA/m) has amounted to $\Delta Z/Z(H_{max}) = 173\%$ at a frequency of 20.46 MHz. The MI curve measured up to 20 MHz shows some shoulder indicating the growth of rotational contribution of magnetization that appears above the domain wall relaxation frequency. The MI profile at frequencies higher than 30 MHz, exhibits a clear peak positioned at transverse anisotropy field H_k, suggesting domination of rotation magnetization in transverse permeability. The linearity in the range up to 5 kA/m with sensitivity of about 11 %/kA/m was observed.

Keywords: MI effects**,** MI sensors, Amorphous alloys, Magnetic field.

1 Introduction

Very interesting phenomena observed in amorphous soft magnetic materials (ribbons/wires or thin films) is magneto-impedance (MI) effect. This effect is manifested by significant changes in the impedance of MI-element under the influence of an external dc magnetic field (H). If magneto-impedance ratio is higher than 100 % it is giant magneto-impedance (GMI) effect. MI effect was discovered in the early nineties of the twentieth century [1] and nowadays it is used for making a very sensitive magnetic field sensor whose sensitivity reaches up to about 7%/(A/m) [1 – 4]. Similar effect is giant magneto-resistive (GMR) effect with the changes of electrical resistance but with lower sensitivity of about 0.0125 %/(A/m) [4]. It should be noted that there are substantial differences in the origin of magneto-impedance compared to the magneto-resistance (MR) effect [5]. MI and MR effects are used for monitoring

[1]Faculty of Technical Sciences, University of Kragujevac, Svetog Save 66, Čačak, Serbia; E-mails: ekorade@gmail.com, nebojsa.mitrovic@ftn.kg.ac.rs, slobodan.djukic@ftn.kg.ac.rs
[2] Military Technical Institute, Ratka Resanovića 1, Belgrade, Serbia; E-mail: vedran.ibrahimovic@gmail.com

magnetic fields as well as induction sensors, magneto – optical sensors, Hall sensors and resonance magnetometers.

Magneto-impedance effect is usually studied with the amorphous and nano-crystalline alloys (in the form of ribbons or wires) obtained by rapidly quenching of the alloy melt onto a rotating copper disc ("melt-spinning roller casting").

Empirical rules for obtaining amorphous structures are as follows:

1. The alloy contains at least three components;
2. The alloy elements should have different atomic diameters (minimum difference of 12 %) whose heat of mixing is almost zero;
3. Metal component should have a negative heat of mixing with metalloids;
4. The standard content of metalloids is about 20 at. %.

The common content of soft magnetic amorphous and nanocrystalline alloys is shown in Fig. 1 [6].

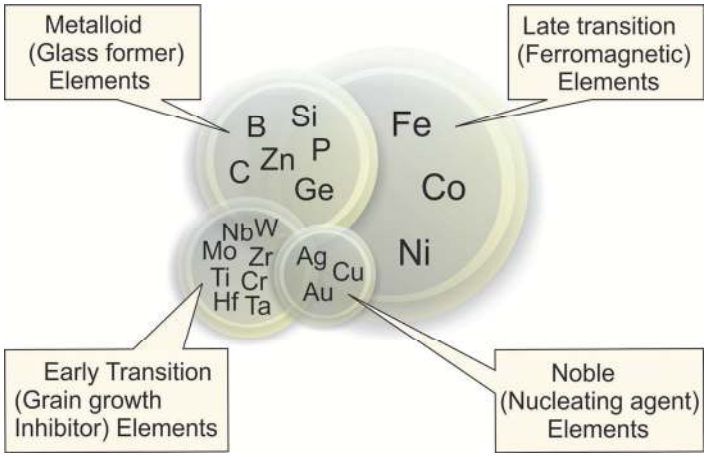

Fig. 1 – *Chemical elements in common soft magnetic amorphous alloys [6].*

Magnetic domains in the ribbon sample are parallelepiped-shaped (see Fig. 2). It can be seen that they are arranged along the y-axis, i.e. at an angle of 90^o in relation to the length of ribbon. Neighboring domains are alternating with the opposite orientation due to achieving the lowest energy configuration. The components of magnetization $\boldsymbol{J}$ along the x-axis and z-axis of the neighboring domains are in opposite orientation too, as it is shown in Fig. 2a [7 – 9].

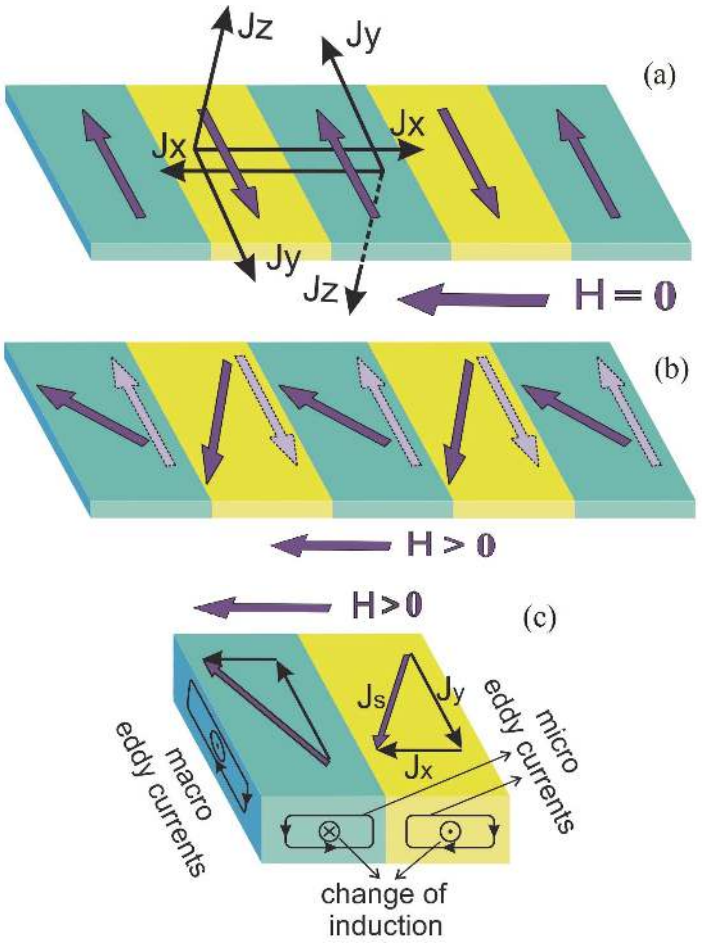

Fig. 2 – *Magnetic domains in amorphous ribbon: appearance (a) for H = 0 [7], (b) for H > 0 [8], and (c) for H >0 showing the micro and macro eddy currents [9].*

Entering sample into external magnetic field is followed by domains rotation according to *x*-axis, i.e. into direction of the magnetic field, thereby reducing impedance of the sample. The effect is more pronounced with the increase of magnetic field intensity. In addition, there is the appearance of negative magnetostriction in width-direction and positive magnetostriction in length-direction of ribbon.

MI-ratio is usually defined as a relative change in the impedance (Z) of a sample under the influence of external DC magnetic field (H):

$$\frac{\Delta Z}{Z}[\%] = 100 \cdot \frac{Z(H) - Z(H_{\max})}{Z(H_{\max})} \quad [\%], \tag{1}$$

where Z (H_{max}) is the impedance at maximum magnetic field that is applied in longitudinal direction of the ribbon sample.

In classical skin-effect explanation, magnetic materials at relatively high frequencies (f) have penetration depth (δ_m) given by:

$$\delta_m = \sqrt{\frac{\rho}{\pi\mu f}} . \tag{2}$$

where: μ is magnetic permeability and ρ is electrical resistivity.

In the soft magnetic material with high permeability and low electrical resistivity at relatively high frequencies, penetration depth becomes less than half of the ribbon thickness, i.e. the radius of wire [10 – 12]. The frequency at which MI-effect starts is evidenced as critical frequency.

It should be also noted that there is an influence of magnetic field on the magnetic permeability, i.e. dependence μ (H). Therefore, at constant frequency changes occur in the impedance of test sample with increase of external DC magnetic field.

2 Experimental

Impedance of the test sample in the form of $Fe_{72}Cu_1V_4Si_{15}B_8$ amorphous ribbon was measured using the Vector Network Analyzer Agilent 8753ES (microwave technique). The application of network analyzer provides more accurate results at higher frequencies in comparison to RLC meter, where impedance is tested by the “four points” method. The MI-element is in the central positon of Helmholtz’s coils with homogeneity of about 99%.

The measuring principle in microwave technology is based on the relationship between the amplitudes of direct wave and reflected wave as shown in Fig. 3. Direct excitation wave was generated from the signal generator. If the origin wave has a different propagation path (different characteristic impedance) the reflection of the excitation wave occurs and the reflected wave is generated. Since the reflected wave occurs due to differences in the impedance, the result of calculation is ratio between the direct and reflected wave, i.e. their amplitudes and phases (S-scattering parameters).

The network analyzer gives measured impedance in the range from 30 kHz to 6 GHz. However, experiments were performed in the frequency range from 30 kHz to 300 MHz, as the maximum MI-ratio is obtained about 25 MHz.

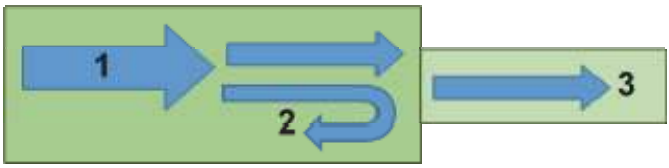

Fig. 3 – *The principle of impedance measurements in the microwave technique, 1 – direct wave, 2 – reflected wave, 3 – wave that passes through the sample.*

In microwave engineering measured response – impedance is equal to the square root of the product of the values measured with open connections and with short circuit, i.e. it is calculated using the formula:

$$Z_x = \sqrt{Z_{oc} Z_{sc}}\ , \tag{3}$$

where is: Z_{oc} – open connections impedance, Z_{sc} – short circuit impedance, Z_x – measured impedance.

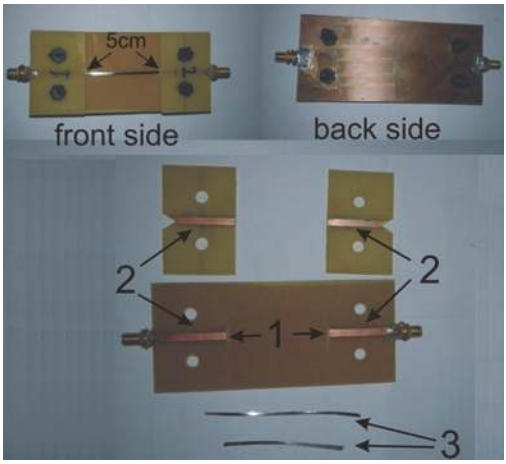

Fig. 4 – *The sample holder and the MI-element: 1 – distance between electrical contacts of MI-element, 2 – sample holder contacts, 3 – samples of tested amorphous ribbons.*

The sample holder is performed by printed circuit board with copper layer on both sides, wherein the upper side contacts are made by bulk copper (Fig. 4). The dimensions are adapted to the length of the ribbon of about 70 mm (the measured length of the sample through the impedance is 50 mm). The sample holder enters into the measuring system some error. In order to eliminate error originated by the sample holder, it is necessary to create short circuit of the holder with copper strip of appropriated dimensions similar to the measured sample, prior to measurement.

Figs. 5 and 6 show an experimental setup for MI measurement that contains power supplies, network analyser Agilent 8753ES and Helmholtz coils.

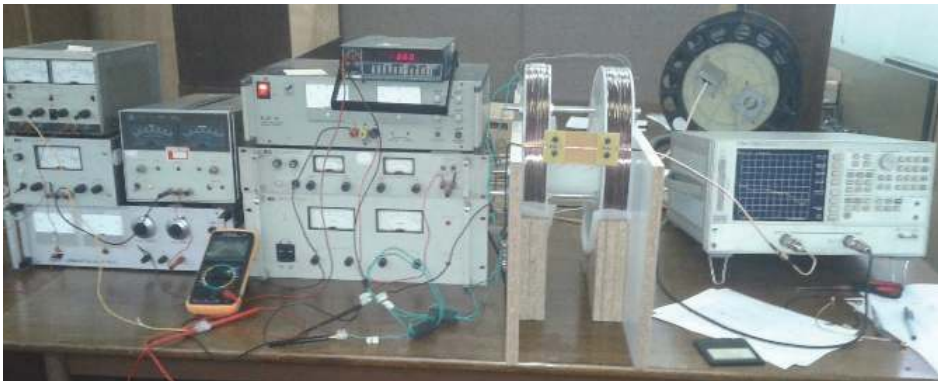

Fig. 5 – *Experimental setup for MI measurement (power supplies, network analyser and Helmholtz coils).*

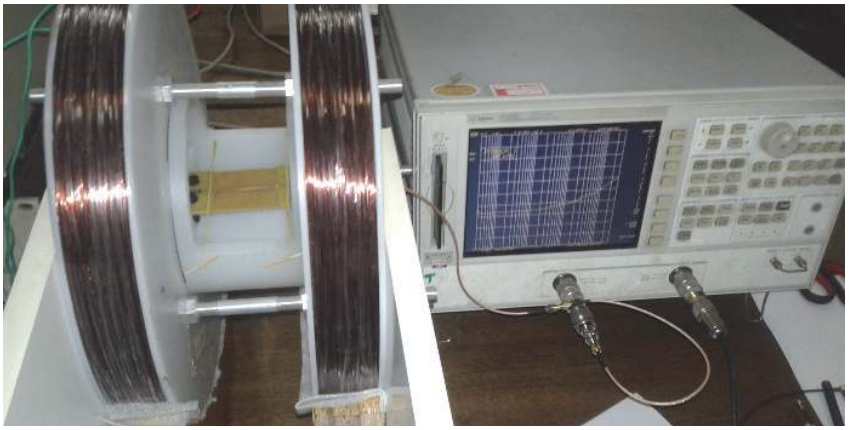

Fig. 6 – *Measuring equipment (Vector Network Analyser and MI-element positioned in Helmholtz coils).*

3 Results and Discussion

Figs. 7 and 8 show the MI-ratio $\Delta Z/Z = (Z(H) - Z(H_{max}))/Z(H_{max})$ vs. frequency with magnetic field intensity H as a parameter. Fig. 7 shows the results of experiments with "positive" direction of magnetic field, while Fig. 8 shows the results of experiments in "negative" direction, i.e. after the exchange of direction. Of course, the maximum of about 173% was observed for maximum $\Delta Z = Z(0) - Z(H_{max})$ at a frequency of 20.46 MHz, as a result of the changes of penetration depth δ_m under the external magnetic field influence.

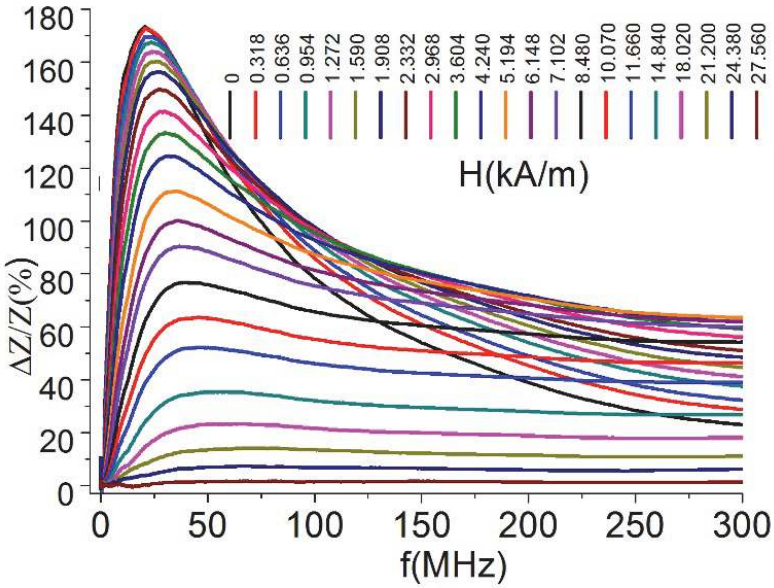

Fig. 7 – *Dependence of the MI ratio on frequency in $Fe_{72}Cu_1V_4Si_{15}B_8$ ribbon („positive" direction of magnetic field).*

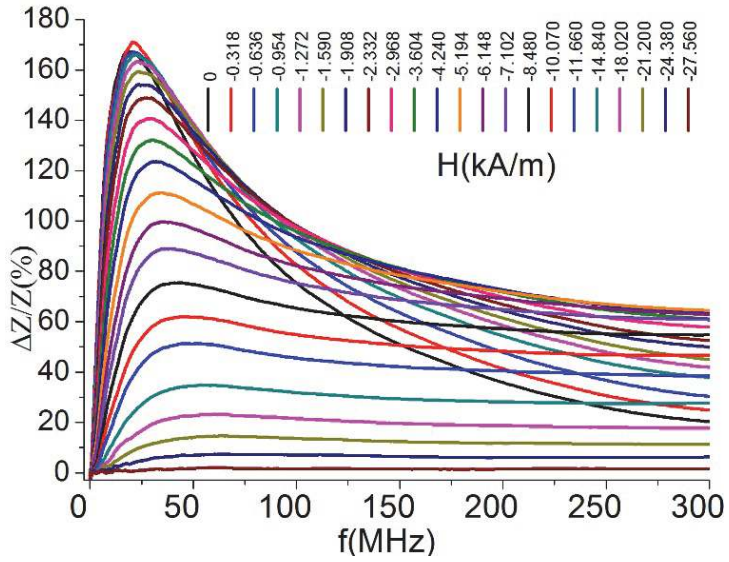

Fig. 8 – *Dependence of the MI ratio on frequency in $Fe_{72}Cu_1V_4Si_{15}B_8$ ribbon („negative" direction of magnetic field).*

The diagram in Fig. 9 presents the MI profile in both magnetic field direction ("positive" and "negative" $H_{max} = \pm 28.6$ kA/m) with driving frequency as a parameter ranging from 1 MHz to 300 MHz. In both cases, the maximum value of impedance was registered at frequency of 20.46 MHz and further increase in frequency is followed with MI-ratio decrease. It is notable symmetry of the observed curves.

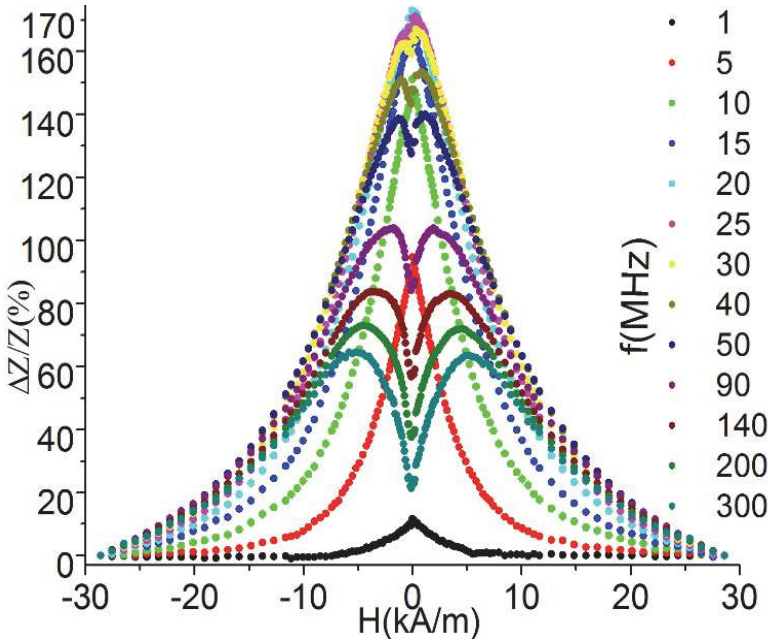

Fig. 9 – *MI profile in $Fe_{72}Cu_1V_4Si_{15}B_8$ ribbon (in both magnetic field direction "positive" and "negative" $H_{max} = \pm 28.6$ kA/m) with driving frequency as a parameter.*

MI profile exhibits the peak positioned at transverse anisotropy magnetic field H_k (see Figs. 9 and 10). This is result of growth of rotational contribution of magnetization in transverse permeability. Dominant influence of mechanism of rotation of magnetization vector during the magnetization process has been observed in the experimental results performed on Co-based ($Co_{70.4}Fe_{4.6}Si_{15}B_{10}$ [13]) and Fe-based ($Fe_{72}A_{15}Ga_2P_{11}C_6B_4$ [14]) soft magnetic ribbons as well as approved by Kraus theory [2].

Furthemore, a shift of the MI-ratio maximum is clearly observed. This increase in transverse magnetic anisotropy field H_k is the most pronounced at frequencies above 30 MHz, as one can see on Fig. 9. Figs. 10, 11 and 12 show calculated MI-ratio performed for different values of maximum external magnetic field H_{max}. The MI ratio exhibits some shoulder indicating the growth

of rotational contribution of magnetization that appears above the domain wall relaxation frequency (see Figs. 10 and 11).

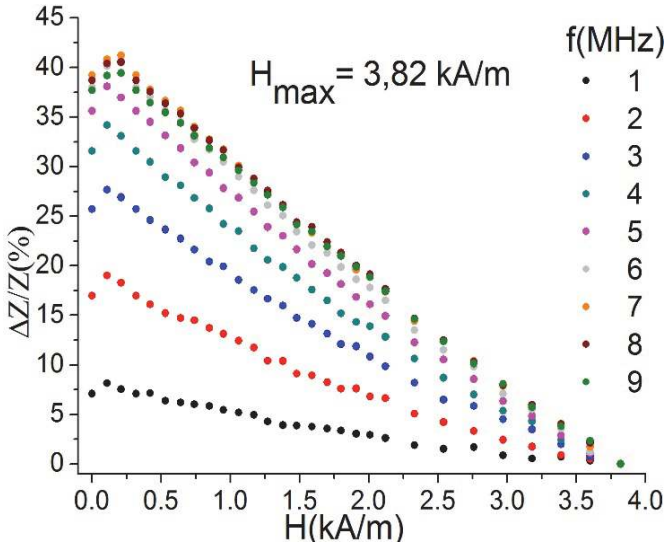

Fig. 10 – *MI ratio in $Fe_{72}Cu_1V_4Si_{15}B_8$ ribbon (H_{max} = 3.82 kA/m) with driving frequency as a parameter, ranging from 1 MHz to 9 MHz.*

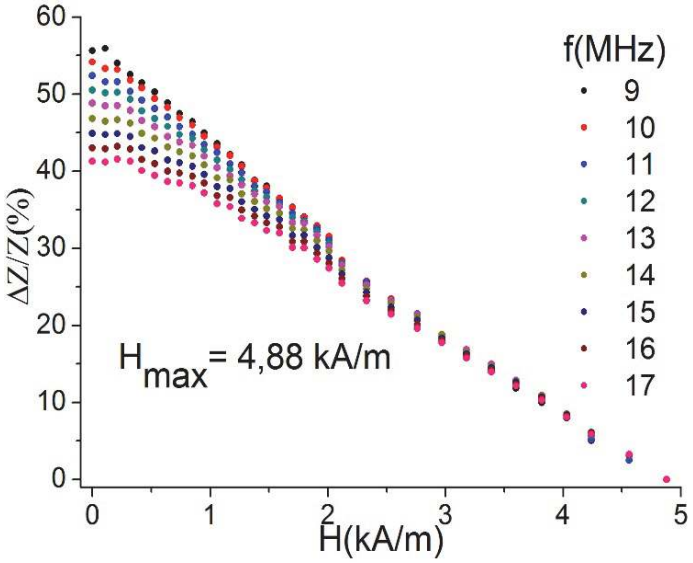

Fig. 11 – *MI ratio in $Fe_{72}Cu_1V_4Si_{15}B_8$ ribbon (H_{max} = 4.88 kA/m) with driving frequency as a parameter, ranging from 9 MHz to 17 MHz.*

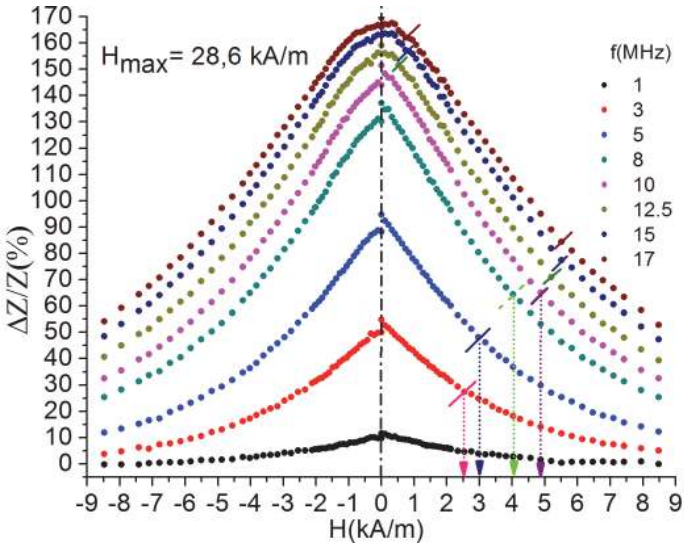

Fig. 12 – *The linearity of MI ratio in $Fe_{72}Cu_1V_4Si_{15}B_8$ ribbon (H_{max} = 28.6 kA/m) with driving frequency as a parameter, ranging from 1 MHz to 17 MHz.*

After the initial increase and peaks positioned at H_k, it can be noticed that linear decrease of MI ratio is within frequency range from 1 MHz to 17 MHz. Analysis performed for low external magnetic fields (H_{max} < 5 kA / m) shows maximum in sensitivity of about 11 %/(kA/m) at frequencies 7–8 MHz.

Fig. 13 shows MI-ratio with driving frequency as a parameter, ranging from 50 MHz to 300 MHz. It presents a clearly visible shift of the maximum value of MI-ratio with increasing frequency (Fig. 13a), i.e. increasing of the magnetic anisotropy field H_k (when $|\Delta Z| = |Z(H) - Z(H_k)| = 0$; Fig. 13b). Opposite to low frequencies, MI-ratio exhibits linearity for low values of the external magnetic field (H_{max} < 3 kA/m). The highest sensitivity of about 7 %/(kA/m) was registered at the frequency of 300 MHz.

Fig. 14 shows 3D diagrams where MI-ratio is presented vs. frequency and external magnetic field, i.e. $(\Delta Z/Z)$ (f, H). Those diagrams enable complete observation of the MI-ratio interdependence on both parameters.

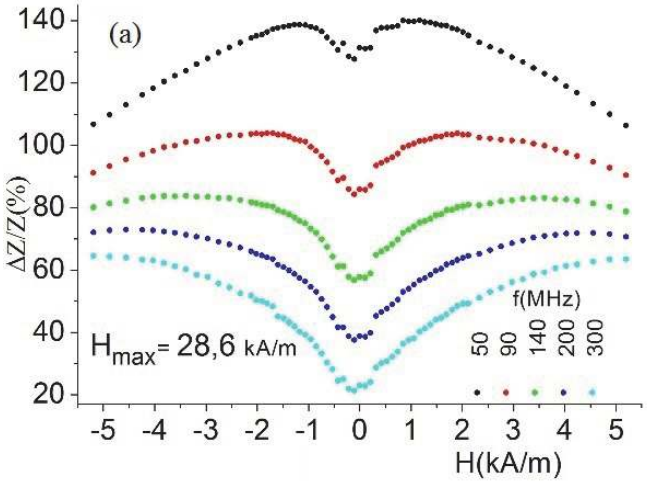

(a)

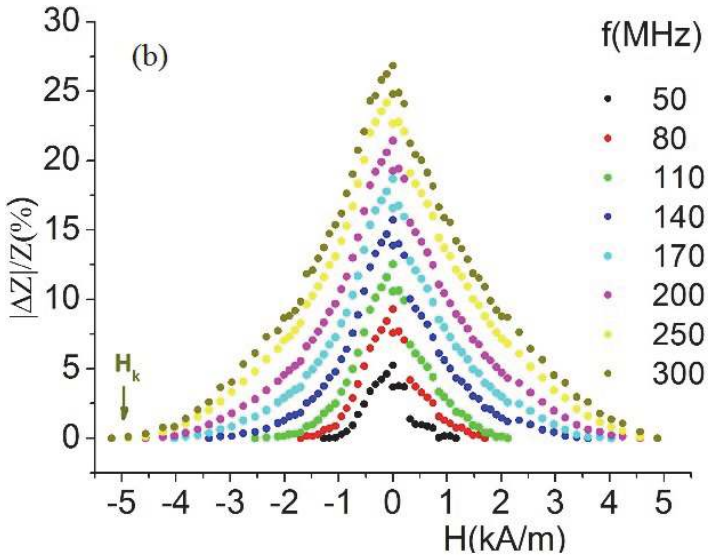

(b)

Fig. 13 – *The linearity of MI ratio in $Fe_{72}Cu_1V_4Si_{15}B_8$ ribbon with driving frequency as a parameter, ranging from 50 MHz to 300 MHz; (a) H_{max} = 28.6 kA/m and (b) $H_{max} = H_к$.*

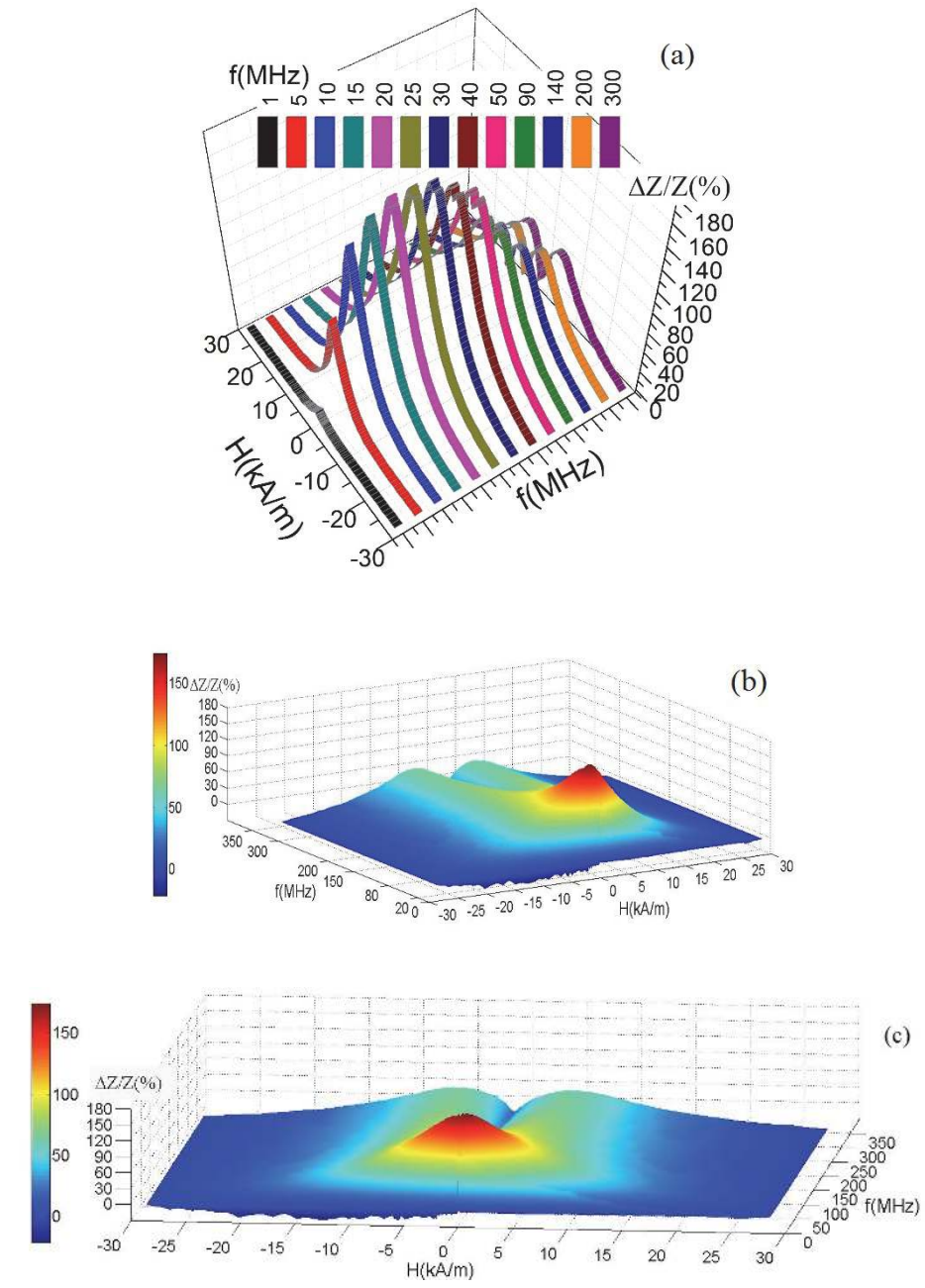

Fig. 14 – *3D diagrams of MI-ratio vs. frequency (range 30 kHz to 300 MHz) and external magnetic field (H_{max} = ± 28.6 kA/m).*

4 Conclusion

The MI effect in $Fe_{72}Cu_1V_4Si_{15}B_8$ soft magnetic amorphous ribbons has been investigated. A maximum of about 173 % (at $H_{max} = 28.6$ kA/m) is obtained by measurements performed by microwave network analysis. A sensitivity of about 11 % / (kA / m) has been observed in the low magnetic field region ($H_{max} \approx 4$–5 kA/m; $f \approx 7$–8 MHz), revealing these ribbons as a potential magnetic field/current sensing MI-elements in the automotive, computer and aerospace industry. Improvement of electrical and magnetic properties of investigated as-cast samples can be attained by structural relaxation after optimal annealing treatment, which will be the subject of next experiments of this alloy ribbons.

5 Acknowledgment

Authors acknowledge the Military Technical Institute Belgrade for technical support. The work was partially funded by the Ministry of Education, Science and Technological Development of Republic of Serbia (Project OI No. 172057).

6 References

[1] L.V. Panina, K. Mohri: Magneto-impedance Effect in Amorphous Wires, Applied Physics Letters, Vol. 65, No. 9, Aug. 1994, pp. 1189 – 1191.

[2] L. Kraus: Theory of Giant Magneto-impedance in the Planar Conductor with Uniaxial Magnetic Anisotropy, Journal of Magnetism and Magnetic Materials, Vol. 195, No. 3, June 1999, pp. 764 – 778.

[3] L. Kraus, Z. Frait, K.R. Pirota, H. Chiriac: Giant Magnetoimpedance in Glass-covered Amorphous Microwires, Journal of Magnetism and Magnetic Materials, Vol. 254–255, Jan. 2003, pp. 399 – 403.

[4] M.H. Phan, H.X. Peng: Giant Magnetoimpedance Materials: Fundamentals and Applications, Progress in Materials Science, Vol. 53, No. 2, Feb. 2008, pp. 323 – 420.

[5] N. Mitrovic: Magnetoresistance of the $Fe_{72}Cu_1V_3Si_{16}B_8$ Amorphous Alloy Annealed by Direct Current Joule Heating, Journal of Magnetism and Magnetic Materials, Vol. 262, No. 2, June 2003, pp. 302 – 307.

[6] R.K. Roy, A.K. Panda, A. Mitra: Alloy Development through Rapid Solidification for Soft Magnetic Application, in Z. Ahmad: New Trends in Alloy Development, Characterization And Application, InTech, Rijeka, Croatia, pp. 40 – 60.

[7] O. Bottauscio, F. Fiorillo, C. Beatrice, A. Caprile, A. Magni: Modeling High-frequency Magnetic Losses in Transverse Anisotropy Amorphous Ribbons, IEEE Transactions on Magnetics, Vol. 51, No. 3, March 2015, p. 2800304.

[8] B. Bergmair, T. Huber, F. Bruckner, Ch. Vogler, M. Fuger, D. Suess: Fully Coupled, Dynamic Model of a Magnetostrictive Amorphous Ribbon and its Validation, Journal of Applied Physics, Vol. 115, No. 2, Jan. 2014, pp. 023905-1 – 023905-10.

[9] G. Herzer: Effect of Domain Size on the Magneto-elastic Damping in Amorphous Ferromagnetic Metals, Zeitschrift für Metallkunde (International Journal of Materials Research), Vol. 93, No. 10, Oct. 2002, pp. 978 – 982.

[10] N. Mitrovic, S. Djukic, A. Rankovic: Optimization of Characteristics of Magnetic Sensor based on Magneto-impedance Effect, XLVI Conference ETRAN, Banja Vrucica-Teslic, BIH, 04-07 June 2002, Vol. 3, pp. 303 – 306. (In Serbian).

[11] S. Djukic, N. Mitrovic, A. Rankovic: The Influence of Structural Relaxation on Magneto-impedance Effect in $Fe_{72}A_{l5}Ga_2P_{11}C_6B_4$ Amorphous Ribbons, XLVIII Conference ETRAN, Cacak, Serbia, 06-10 June 2004, Vol. IV, pp. 226 – 229.

[12] A. Kalezic-Glisovic, N. Mitrovic, A. Maricic, S. Djukic, R. Simeunovic: Study of Stress-Annealing Enhancement of Magnetoimpedance Effect in $Fe_{89,8}Ni_{1,5}Si_{5,2}B_3C_{0,5}$ Metallic Glass Ribbons, Acta Physica Polonica A, Vol. 113, No. 1, Jan. 2008, pp. 103 – 106.

[13] R.L. Sommer, C.L. Chen: Role of Magnetic Anisotropy in the Magnetoimpedance Effect in Amorphous Alloys, Applied Physics Letters, Vol. 67, No. Aug. 1995, p. 857 – 859.

[14] N.S. Mitrovic, S.N. Kane, P.V. Tyagi, S. Roth: Effect of DC-Joule-heating Thermal Processing on Magnetoimpedance of $Fe_{72}A_{l5}Ga_2P_{11}C_6B_4$ Amorphous Alloy, Journal of Magnetism and Magnetic Materials, Vol. 320, No. 20, Oct. 2008, pp. e792 – e796.